

Figure S1. 2D HN correlation spectrum of G53A MPD-ub with resonance assignments. We were unable to unambiguously assign the cross-peaks of several residues, noted below. Unless stated otherwise the reason why these residues were not assigned was that the corresponding cross-peaks in the 3D experiments were either too weak for detection or the corresponding  $^{13}\text{C}$  frequencies did not allow unambiguous assignment.

M1: presumably due to fast solvent exchange also invisible in solution

L8, T9: due to fast transverse relaxation induced by the loop motion (note the fast relaxation of the neighboring G10 and K11).

E16, I23, Q31, Q40.

The cross-peak of residue V5 is overlapped with T66, and H68 overlaps with T7 (not labeled here).

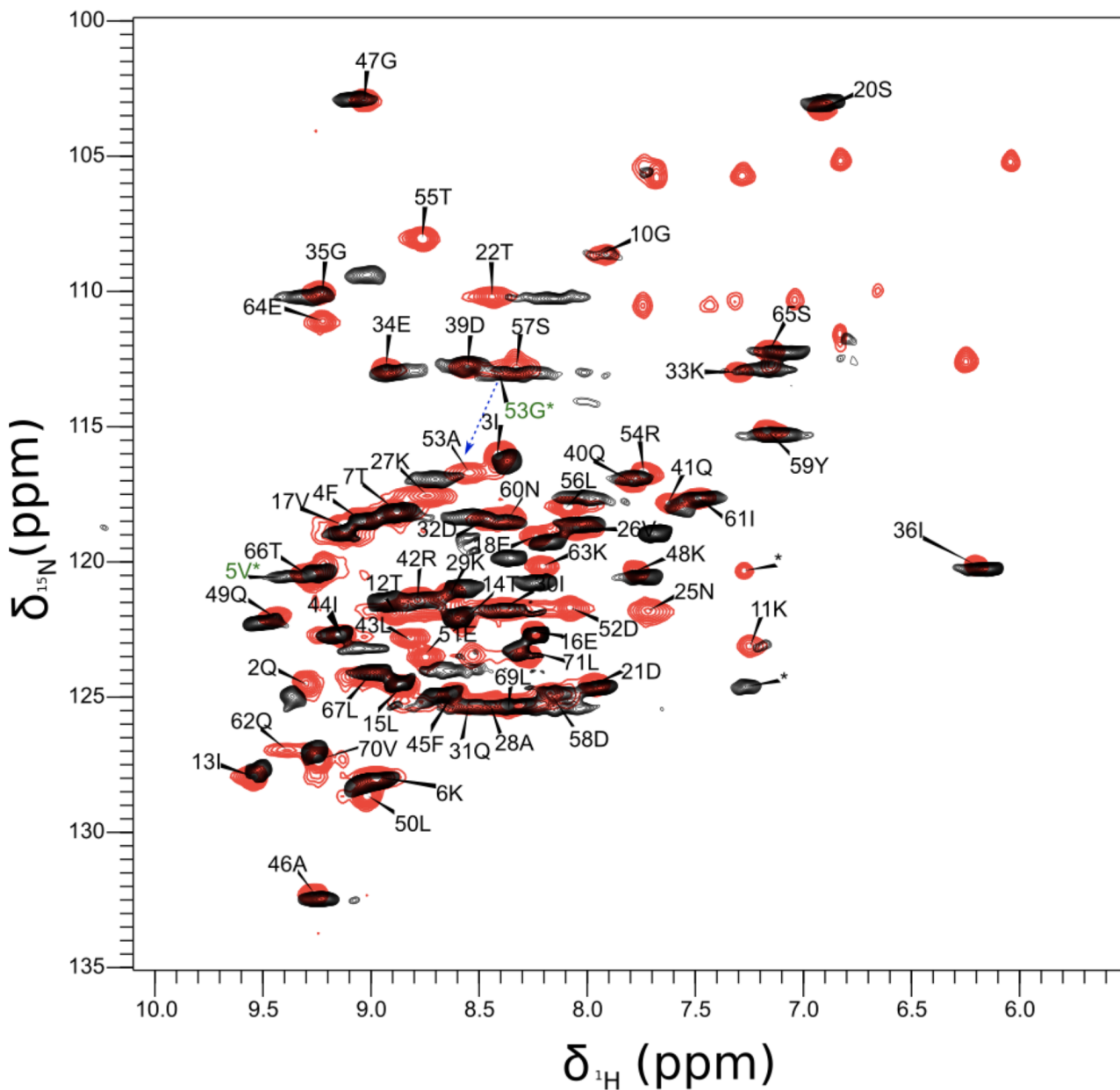


Figure S2. Comparison of HN correlation spectra of WT ubiquitin (black) and G53A ubiquitin (red; the latter is the same as in Figure S1.). The correlation peaks labeled with an asterisk at a  $^1\text{H}$  frequency of 7.25 ppm are aliased in the  $^{15}\text{N}$  dimension.

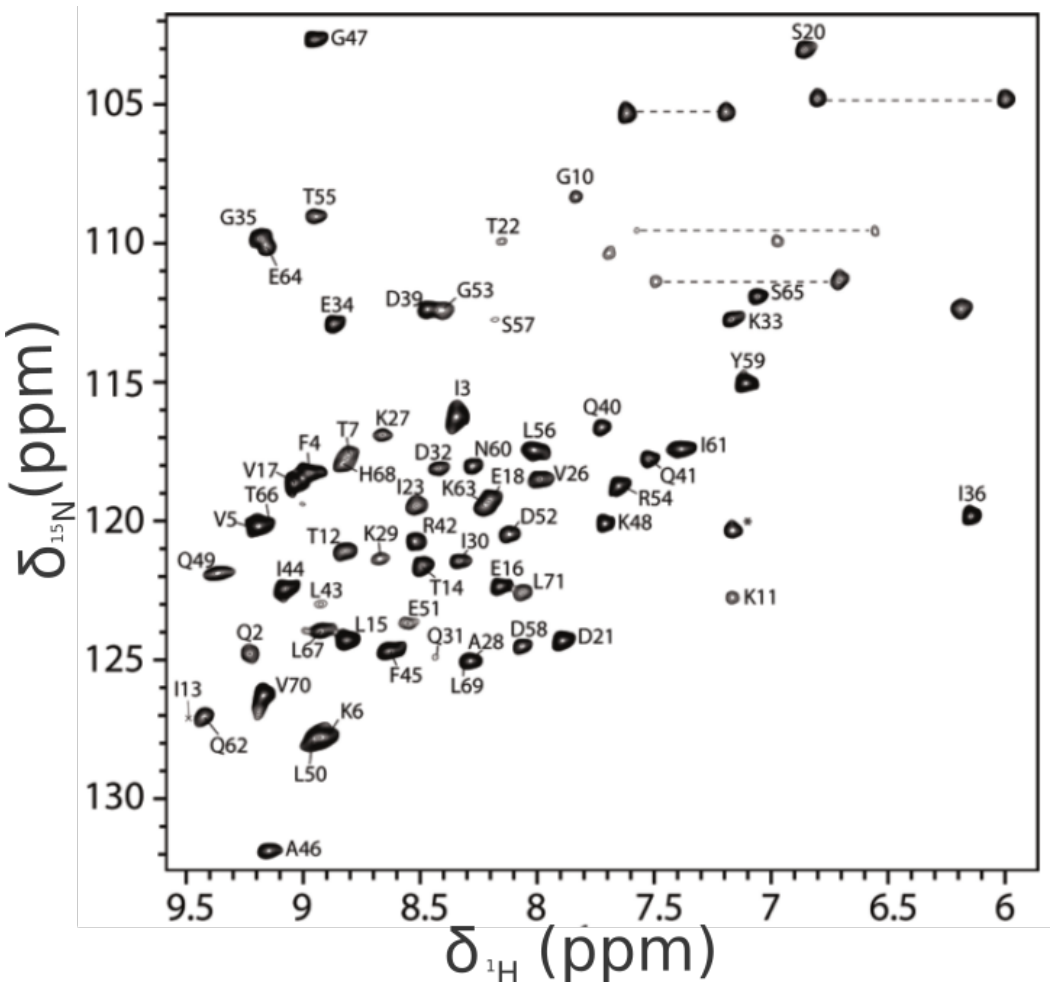


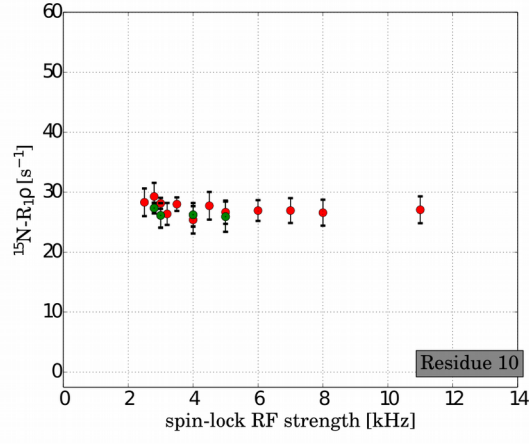
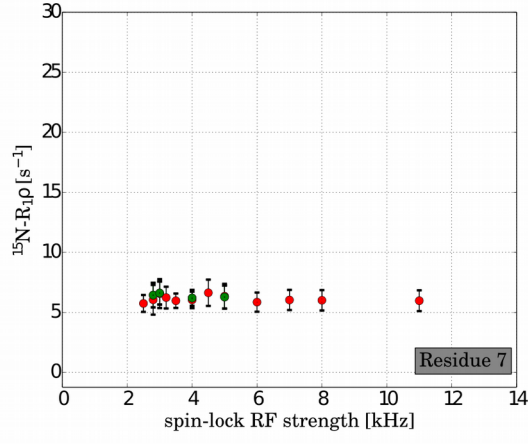
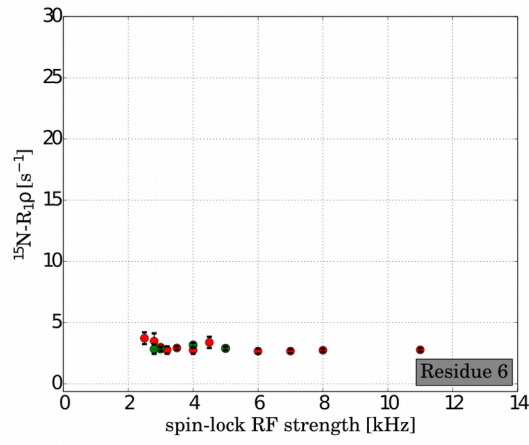
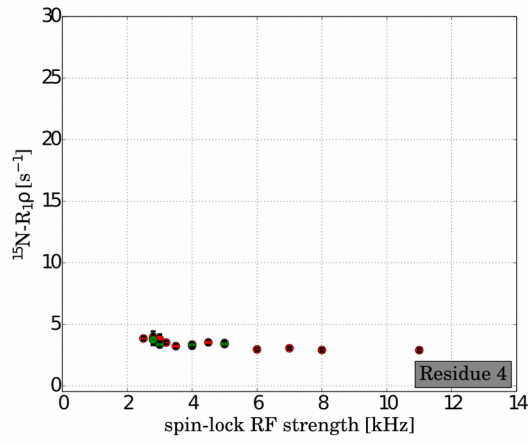
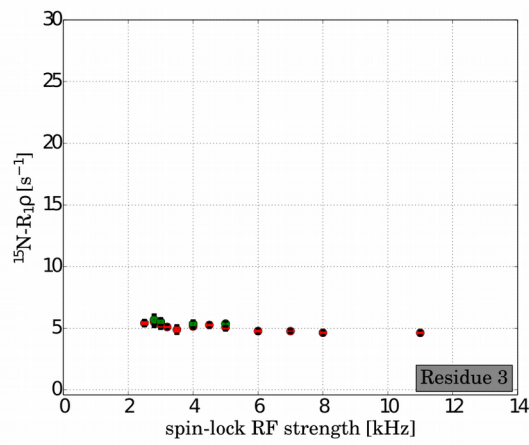
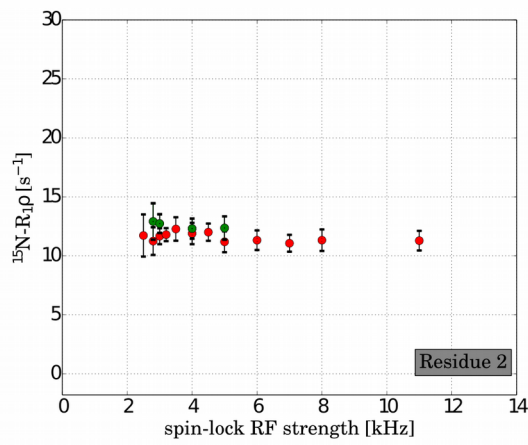
Figure S3. HN correlation spectrum of wild-type ubiquitin, recorded under different conditions (45 kHz MAS, 850 MHz  $^1\text{H}$  Larmor frequency, 301 K sample temperature) and using a different sample than used in this study, as reported in reference:

Schanda, P., Meier, B. H. & Ernst, M. Quantitative Analysis of Protein Backbone Dynamics in Microcrystalline Ubiquitin by Solid-State NMR Spectroscopy. *J. Am. Chem. Soc.* **132**, 15957–15967 (2010).

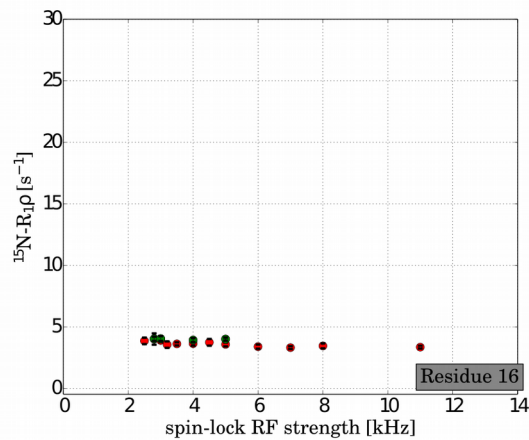
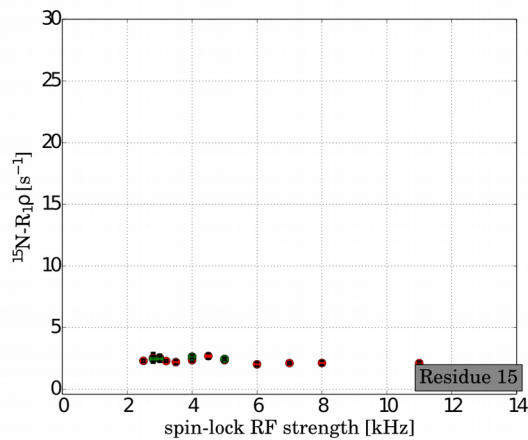
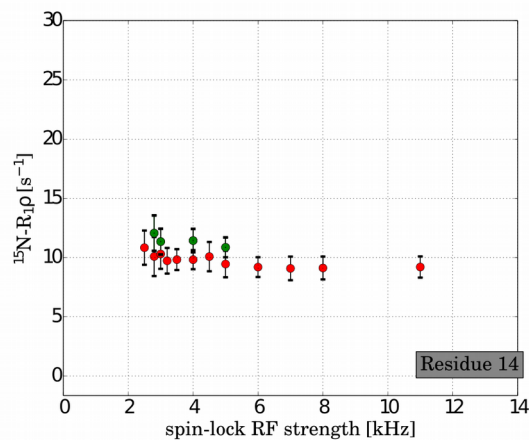
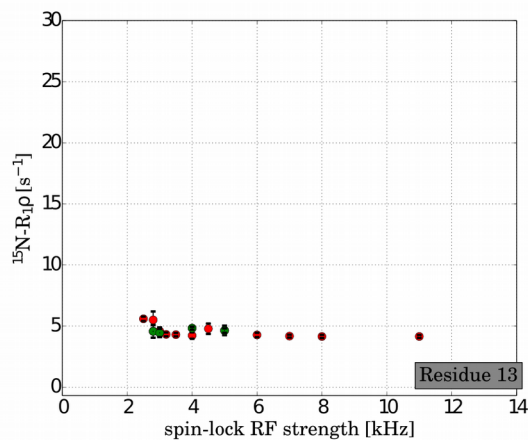
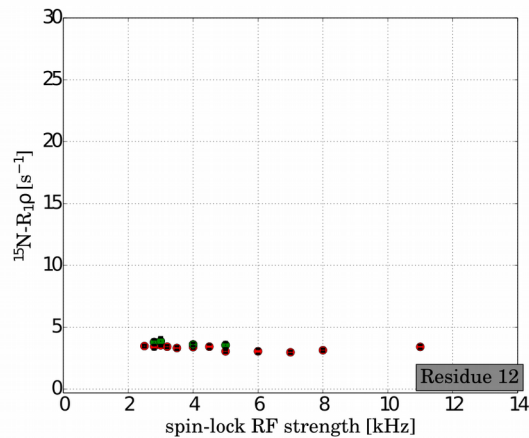
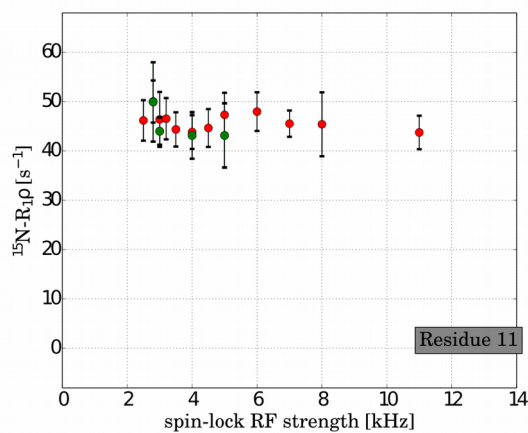
Figure S4, shown on the next ten pages:  $^{15}\text{N}$   $R_{1\text{p}}$  relaxation-dispersion profiles of G53A ubiquitin crystals. See Figure 5 and the main text for details.

In addition to the data shown in the main paper (Figure 5, shown here in red), we have performed another independent experiment, at the same MAS frequency but at a slightly different temperature (ca. 3-5 degrees lower). This experiment was motivated by the realization that there was a small but detectable fluctuation in the  $R_{1\text{p}}$  data point of some residues (a “dip” around 3 kHz, see Figure 5). Although this effect is small and of no practical relevance for the conclusions made in this study, and we wanted to investigate whether this was a reproducible effect. This additional data set, shown as green data points, does not show any sign of fluctuation, excluding any relevant systematic effect. The new data set differs primarily for those residues which undergo conformational exchange, and this finding further confirms the dynamic (and therefore temperature-dependent) origin of these relaxation dispersion profiles.

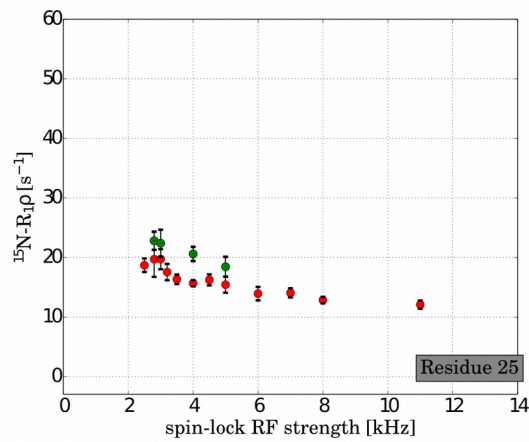
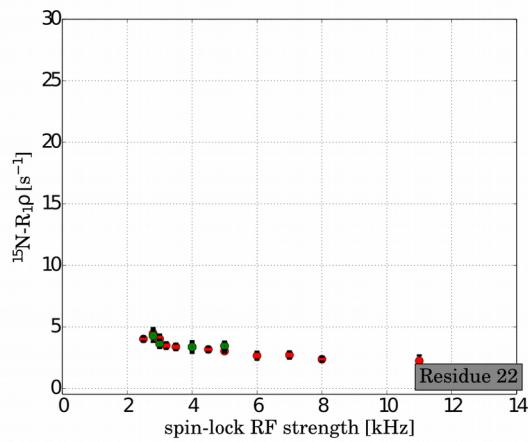
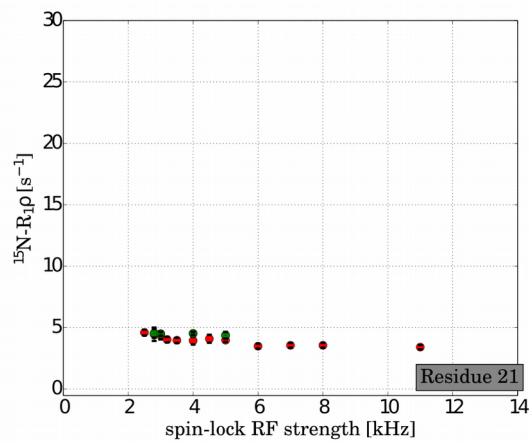
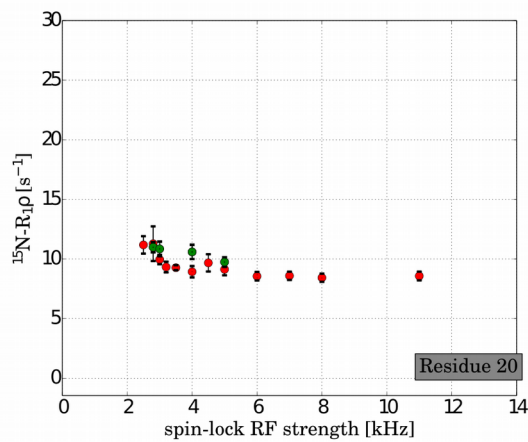
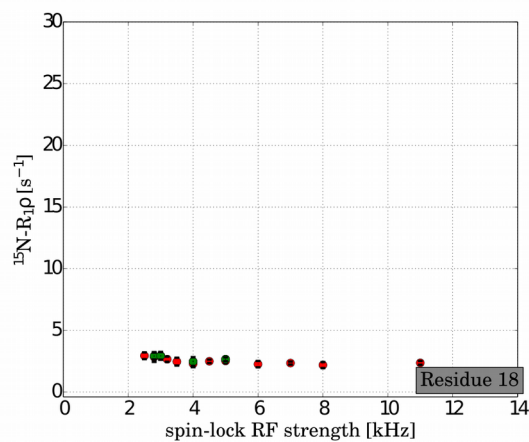
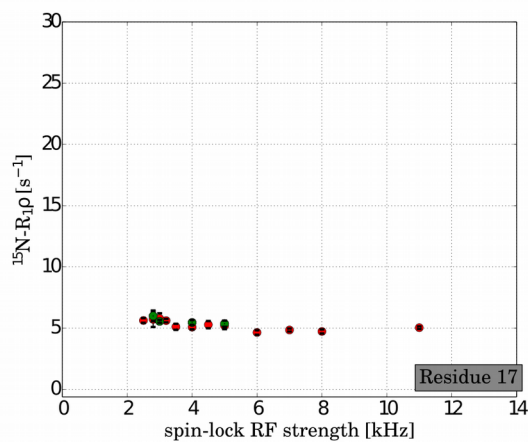
**Figure S4 (continued on next pages)**



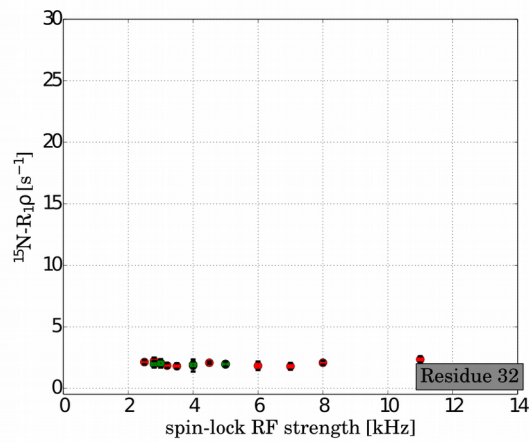
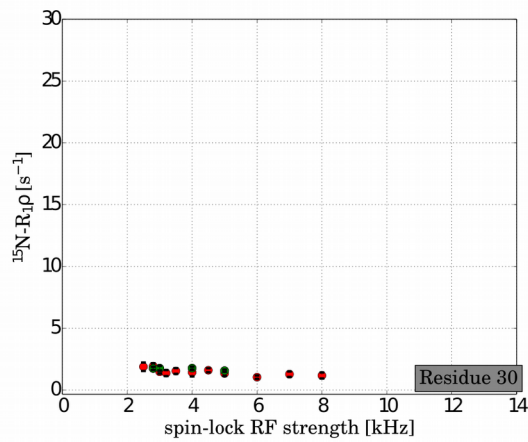
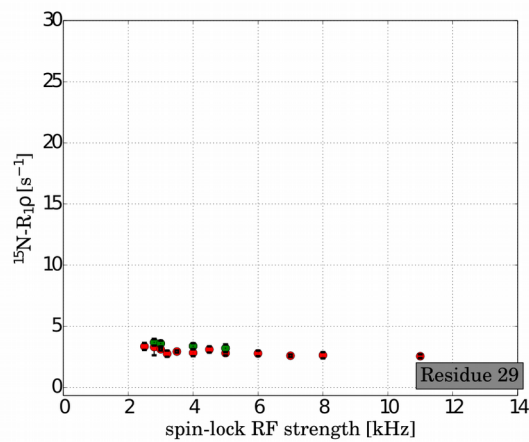
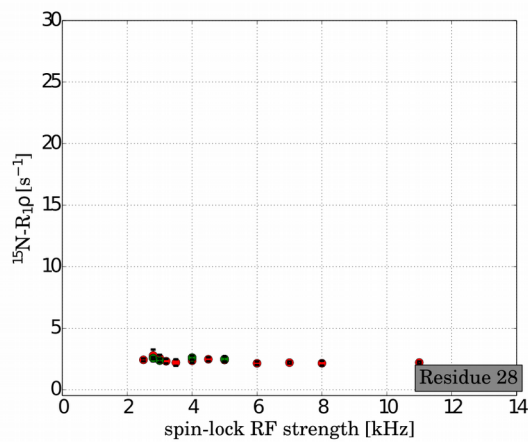
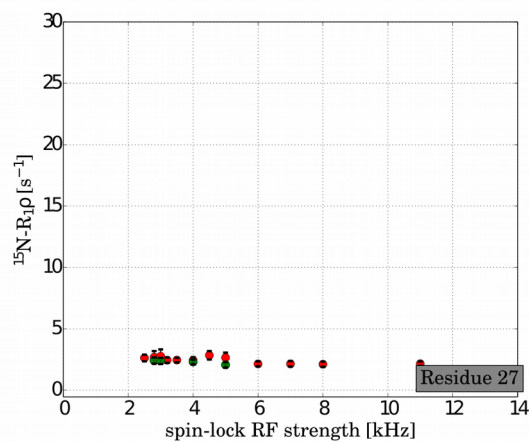
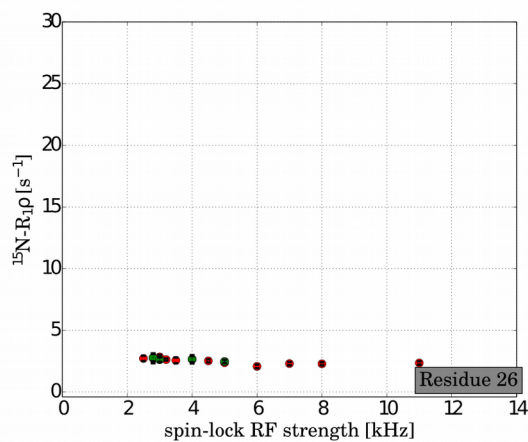
**Figure S4 (continued)**



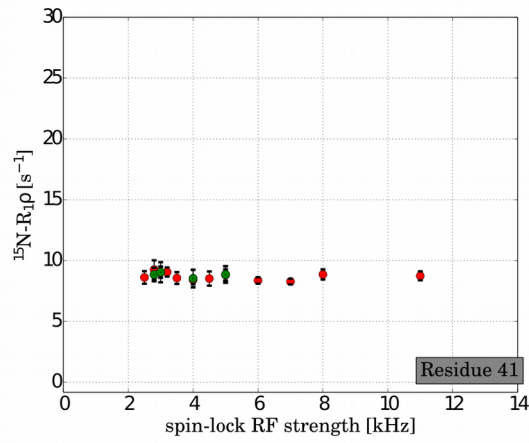
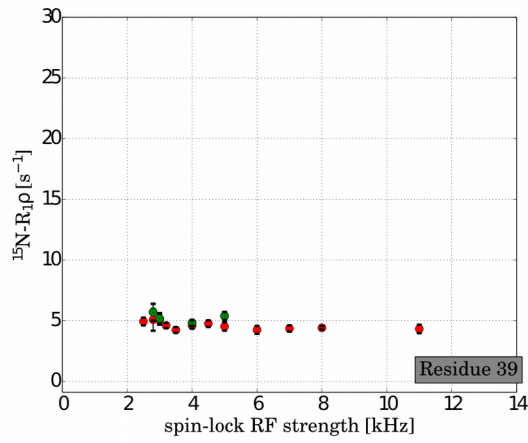
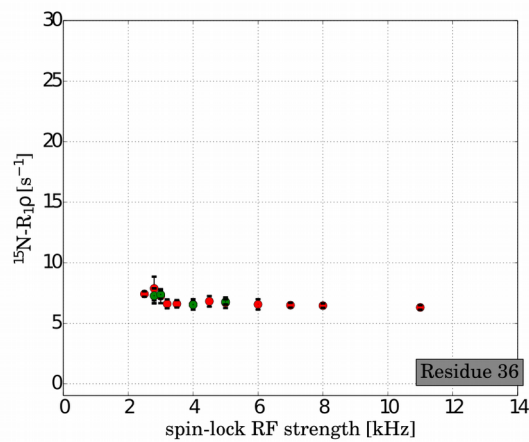
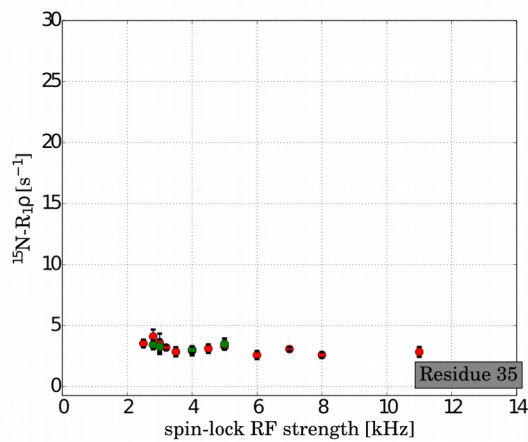
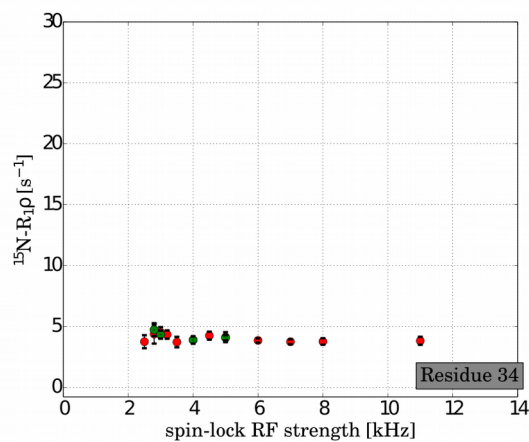
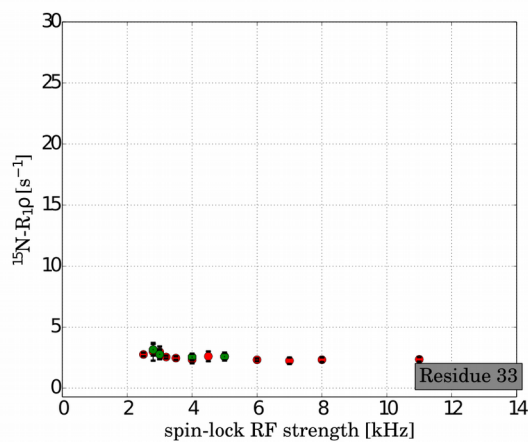
**Figure S4 (continued)**



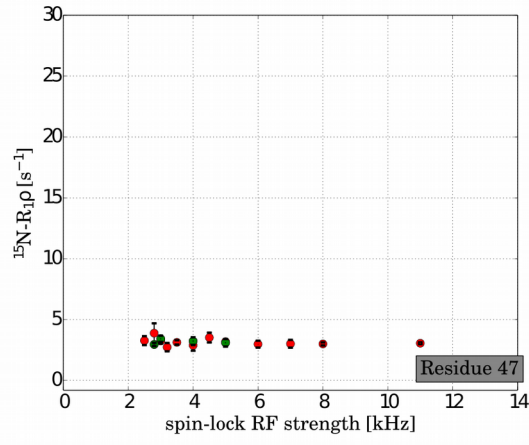
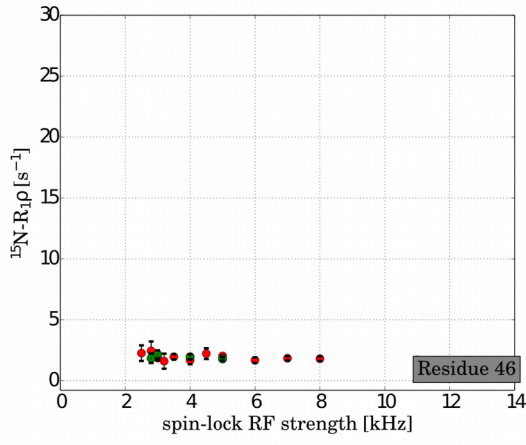
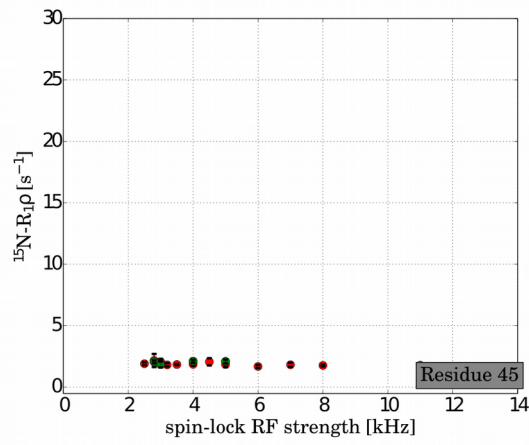
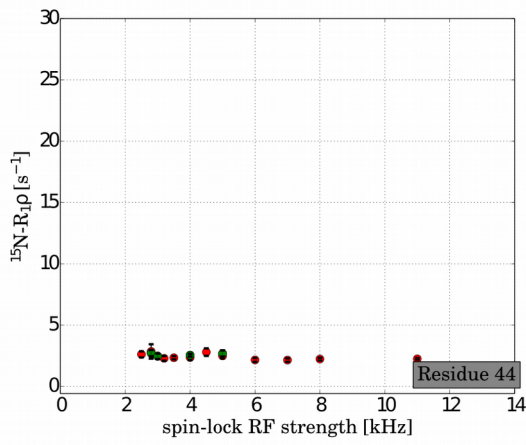
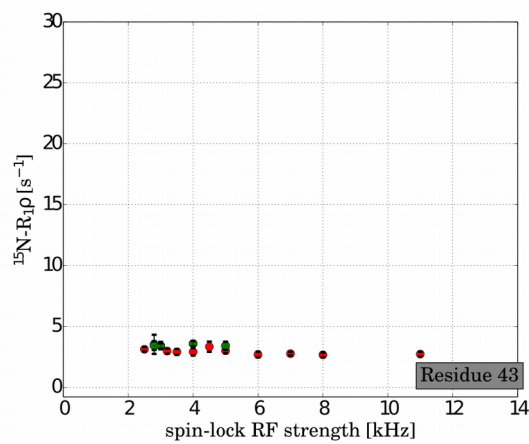
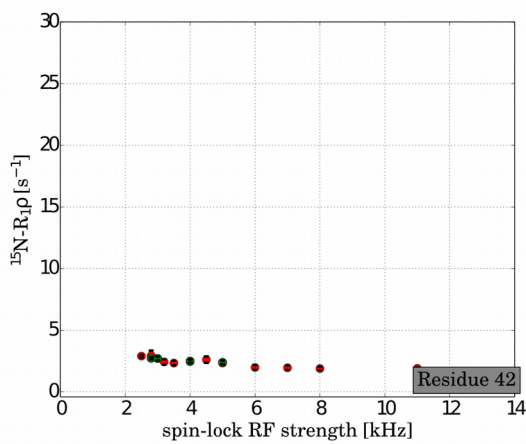
**Figure S4 (continued)**



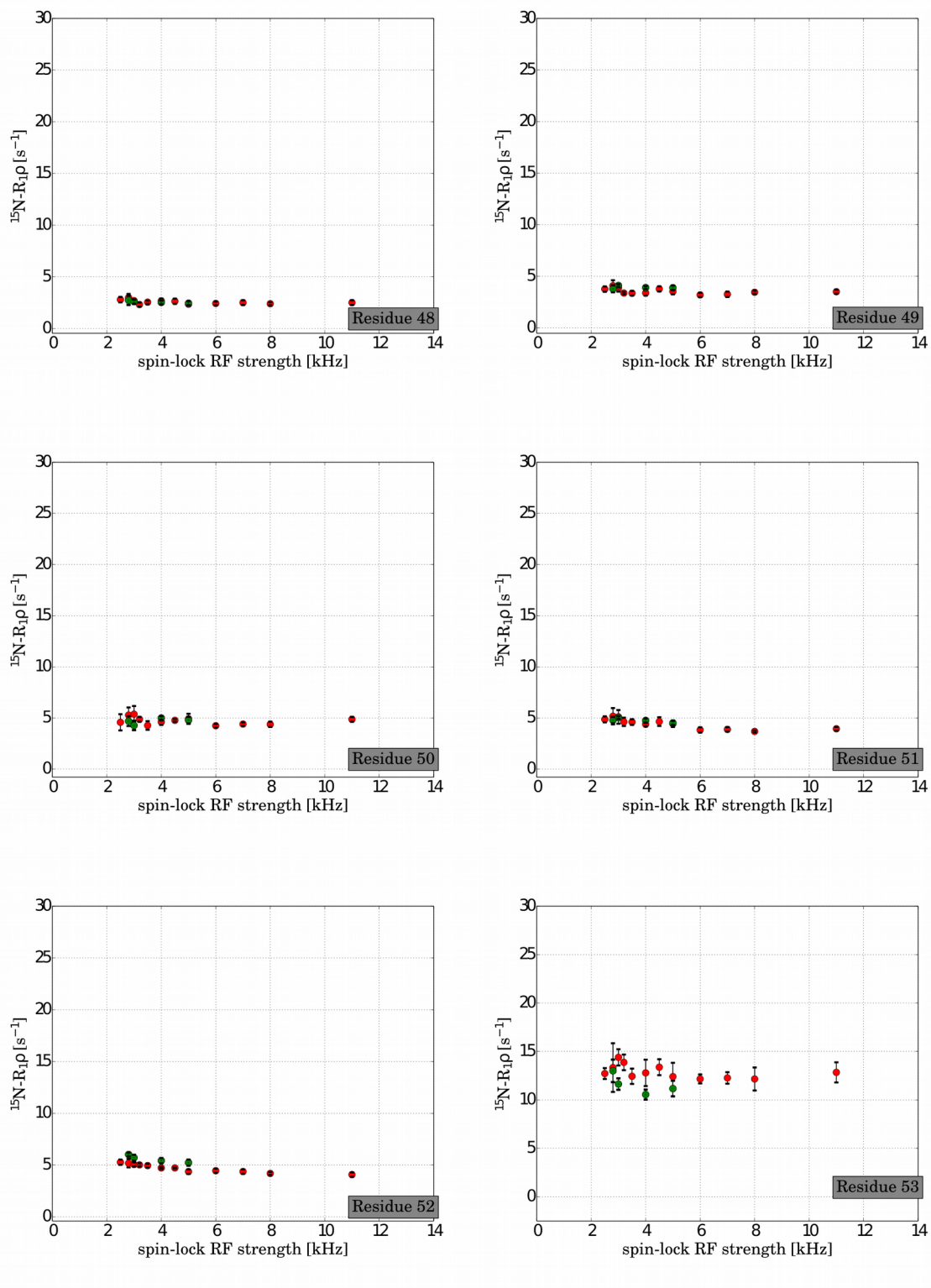
**Figure S4 (continued)**



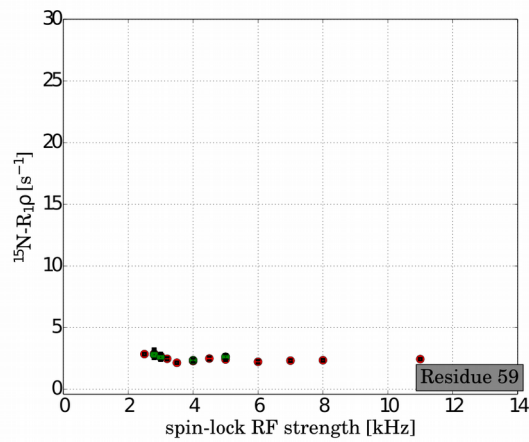
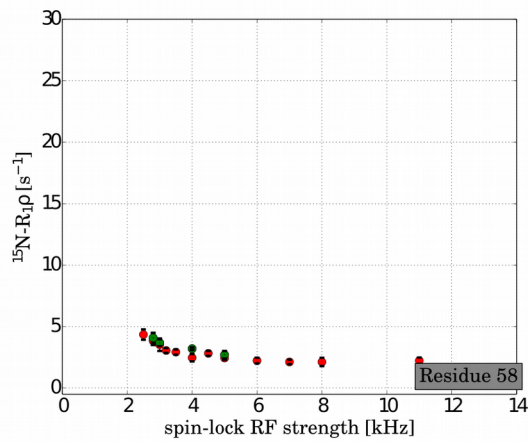
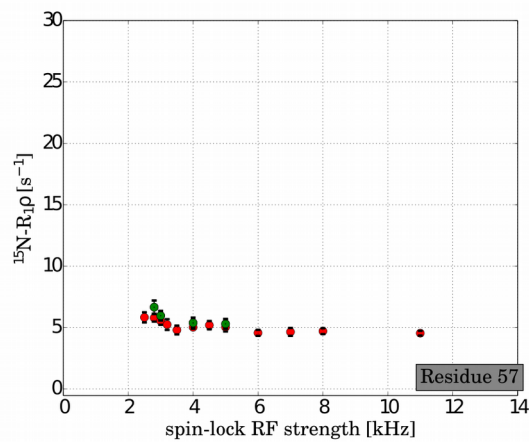
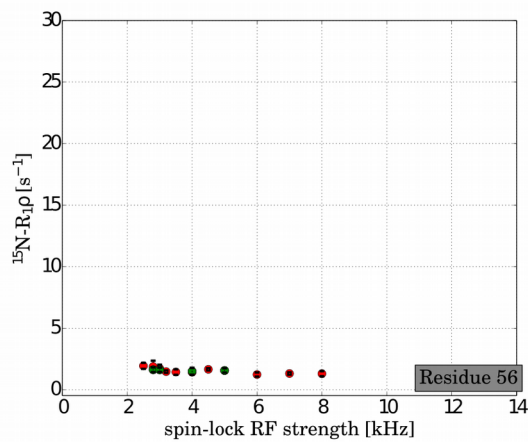
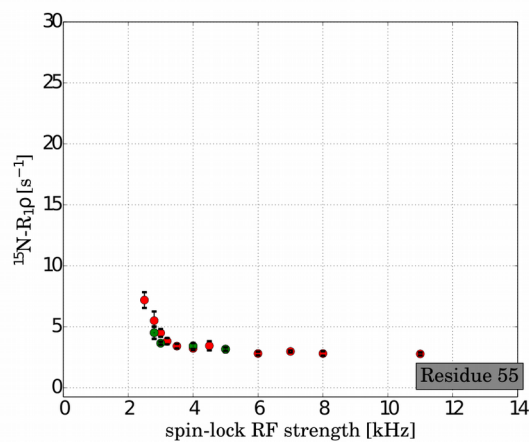
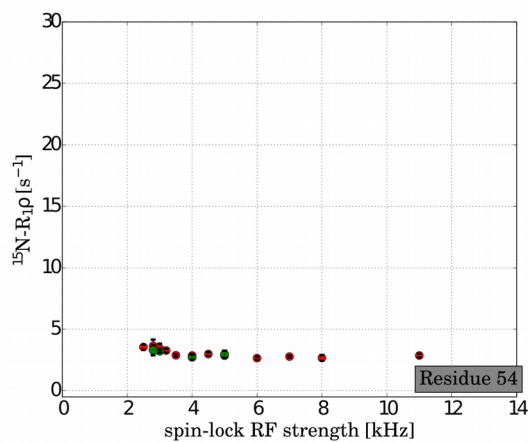
**Figure S4 (continued)**



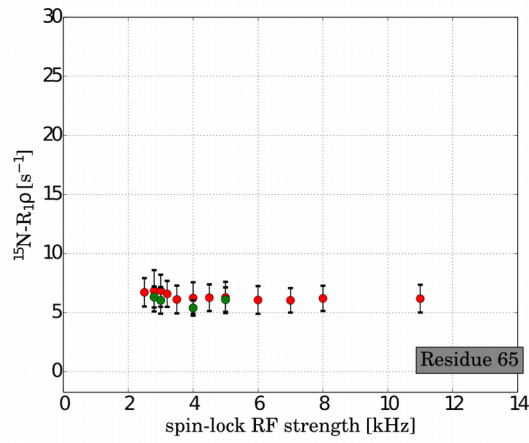
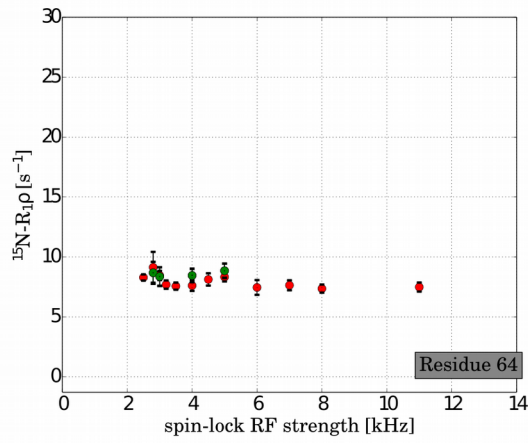
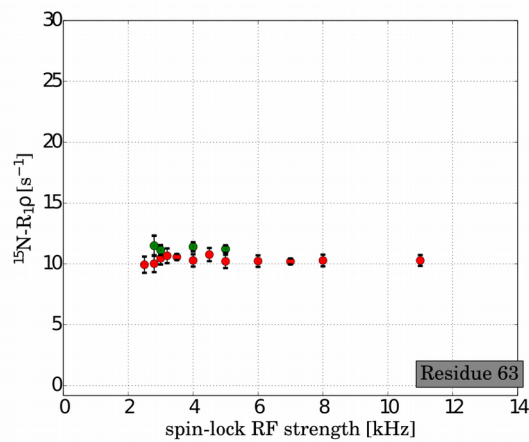
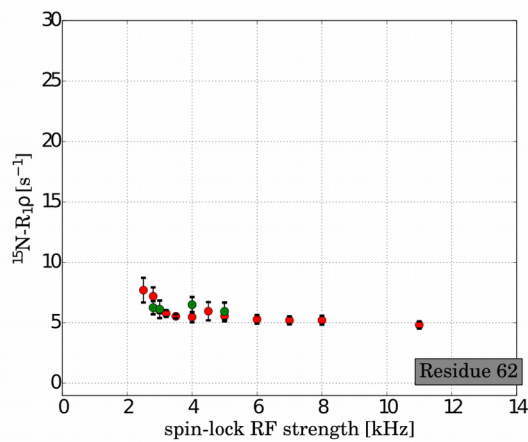
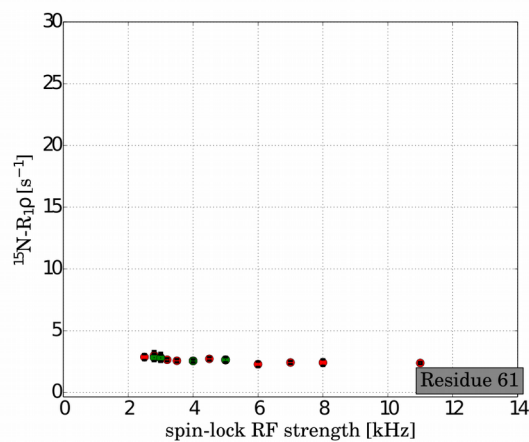
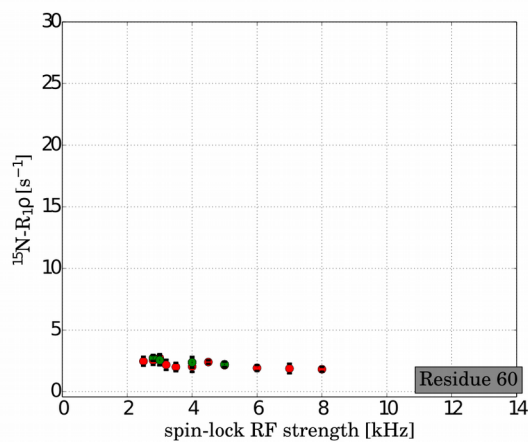
**Figure S4 (continued)**



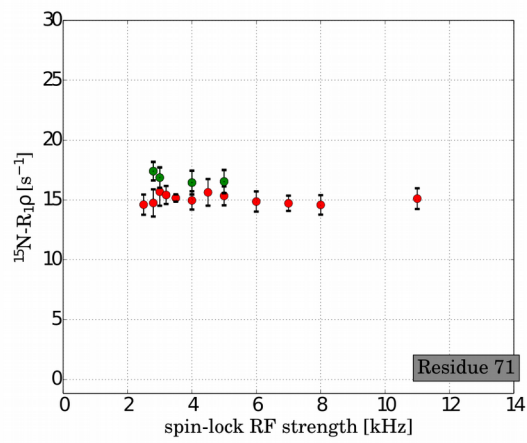
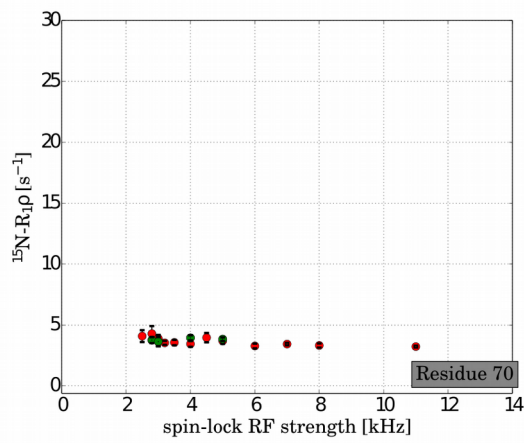
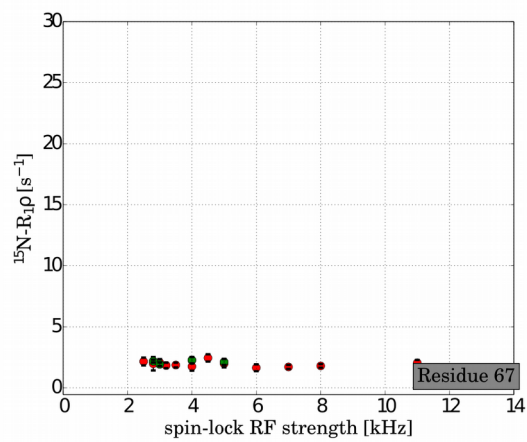
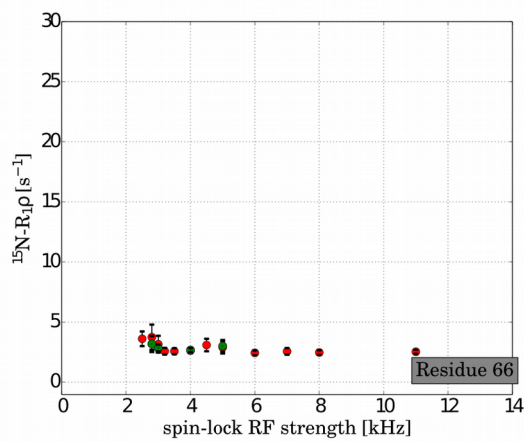
**Figure S4 (continued)**



**Figure S4 (continued)**



**Figure S4 (continued)**



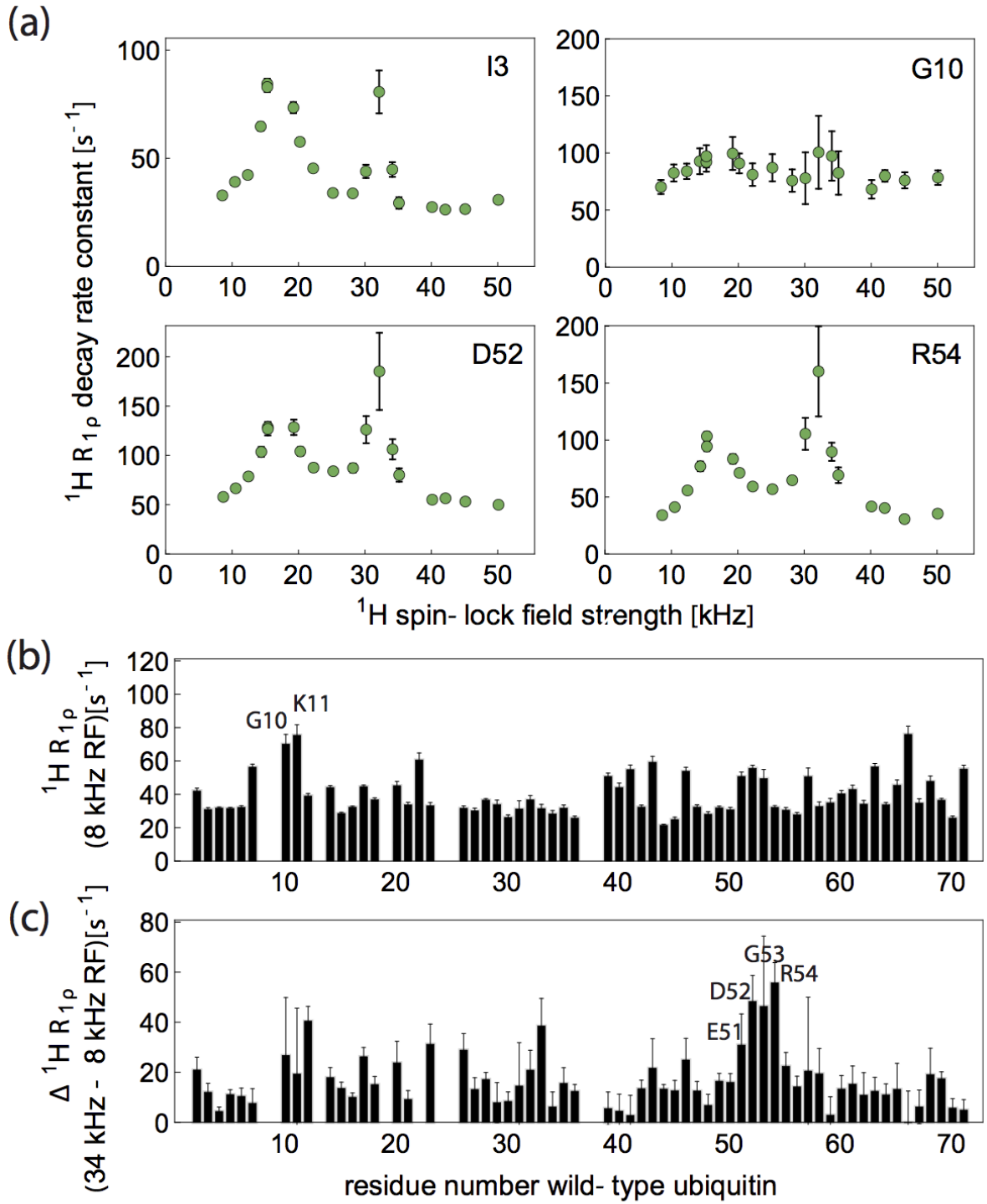


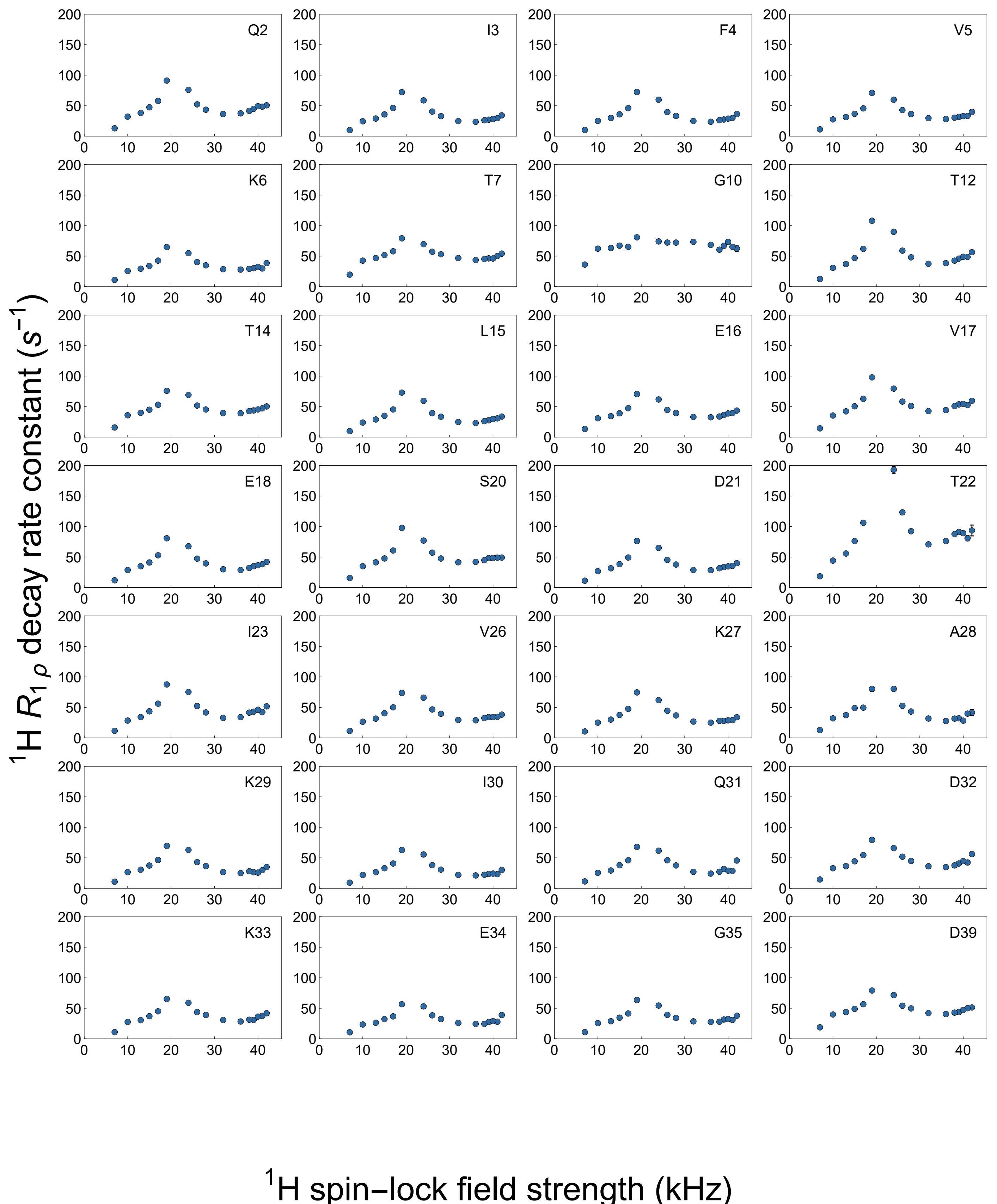
Figure S5.  ${}^1\text{H } \text{R}_{1\text{p}}$  relaxation data obtained with a sample of wild-type ubiquitin which was re-protonated at exchangeable sites to 35% and deuterated otherwise, performed at a MAS frequency of 35 kHz and a  ${}^1\text{H}$  Larmor frequency of 800 MHz. This figure is the equivalent of Figure 8 of the main paper, at a different  $B_0$  field strength. (a) Example relaxation dispersion profiles, i.e.  ${}^1\text{H } \text{R}_{1\text{p}}$  as a function of the applied RF field strength, for four selected residues (all residues are shown in Figure S6). (b) Residue-wise values of  ${}^1\text{H } \text{R}_{1\text{p}}$  rate constants obtained using a  ${}^1\text{H}$  RF spin-lock field strength of 8 kHz. (c) Difference of the rate constants obtained with 34 kHz RF field strength and 8 kHz RF field strength, providing a rapid qualitative view which residues show the largest dispersion effects. As expected from the known microsecond mobility in this region, residues in the  $\beta$ -turn show the largest effects.

Figure S6 and Figure S7, both of which span two pages, are shown on the next four pages:

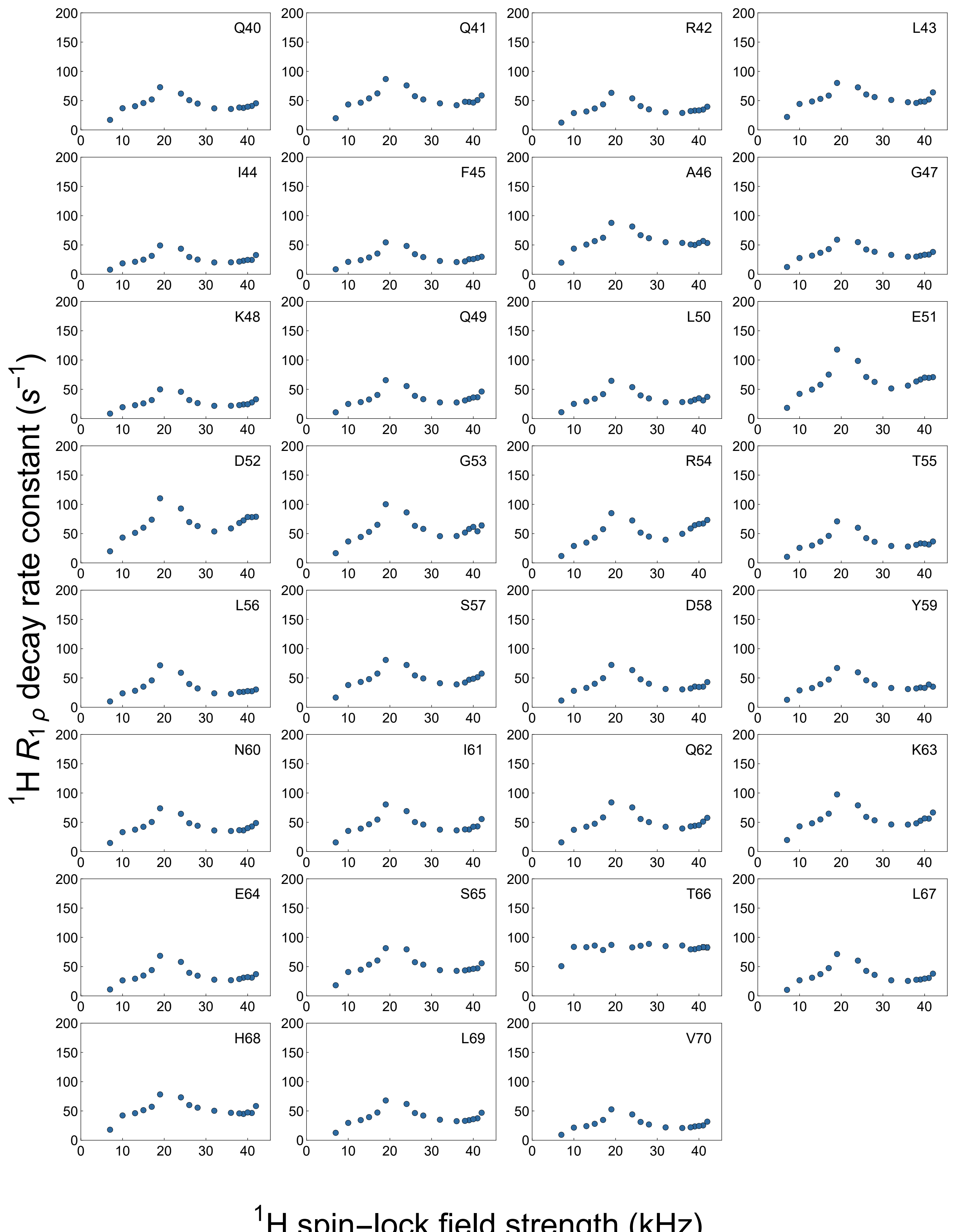
Figure S6. All  $^1\text{H}$   $R_{1\text{p}}$  relaxation data obtained with wild-type ubiquitin crystals at 44.053 kHz and 600 MHz  $^1\text{H}$  Larmor frequency. See Figure 8 text for details.

Figure S7. All  $^1\text{H}$   $R_{1\text{p}}$  relaxation data obtained with wild-type ubiquitin crystals at 35 kHz and 800 MHz  $^1\text{H}$  Larmor frequency. This figure extends on the data shown in Figure S4.

**Figure S6 (continued on next page)**

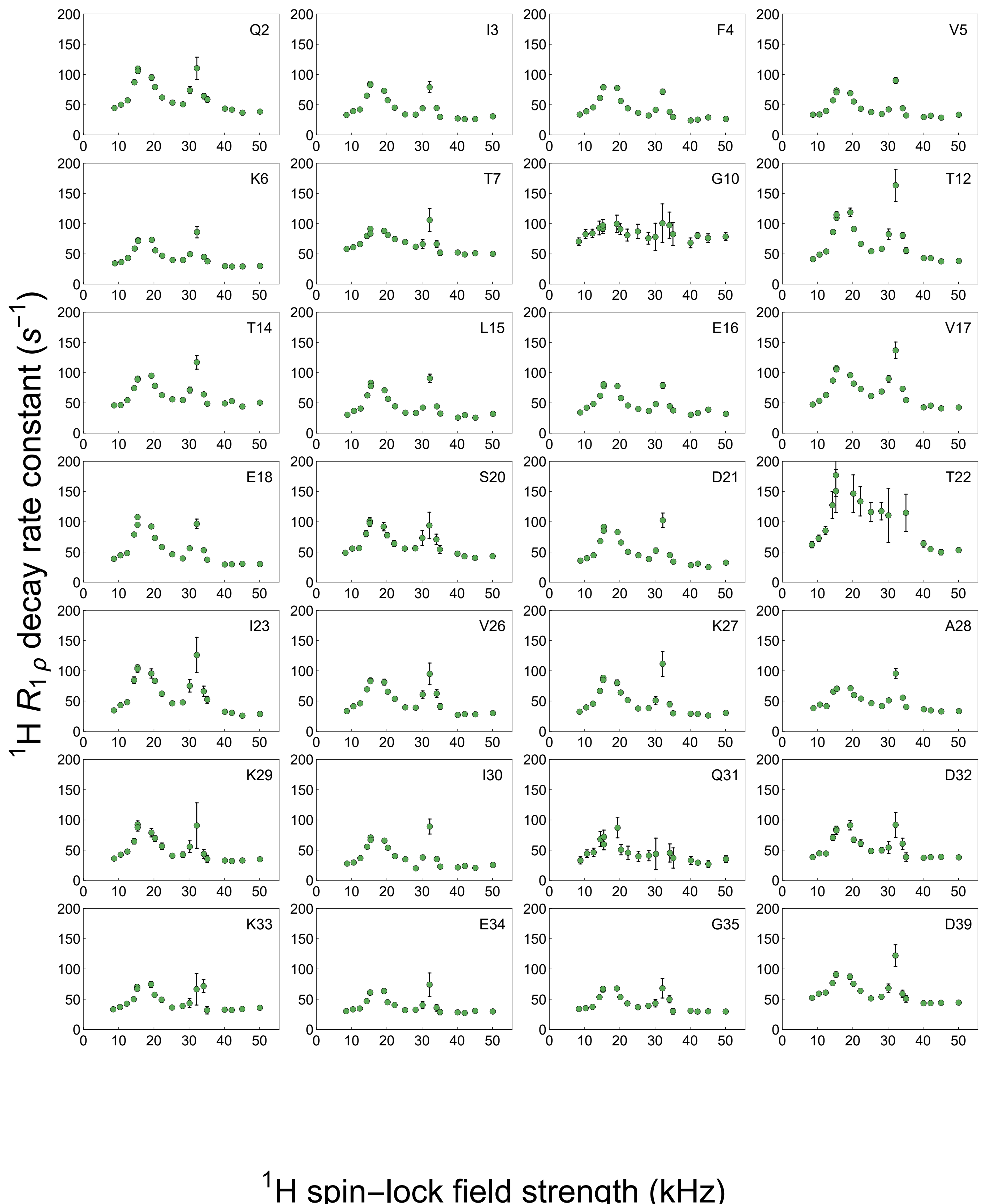


**Figure S6 (continued)**

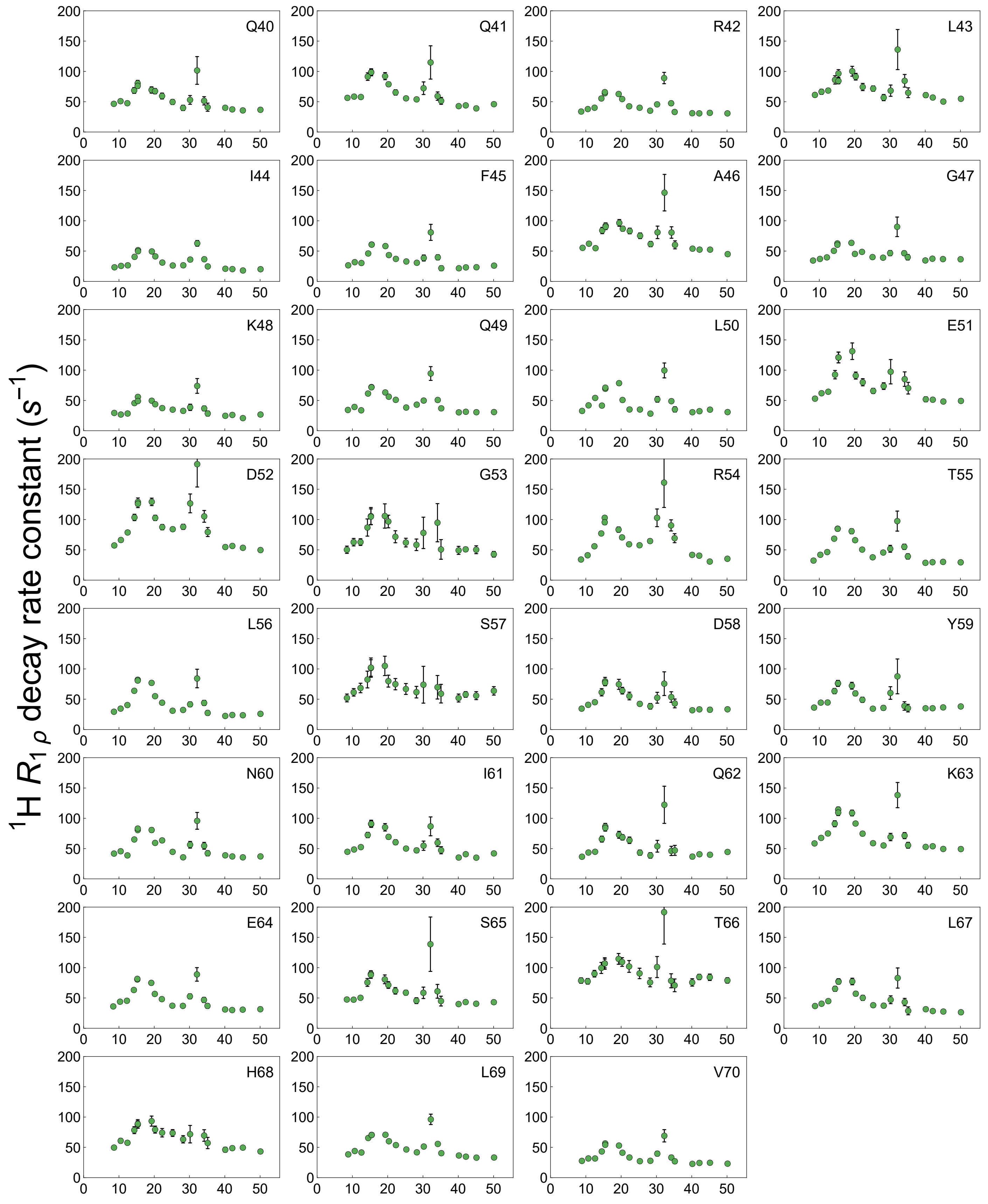


${}^1\text{H}$  spin-lock field strength (kHz)

**Figure S7 (continued on next page)**



**Figure S7 (continued)**



${}^1\text{H}$  spin-lock field strength (kHz)